

Ionic Structure Analysis of Relaxed Surface of Molten Oxide Slags for Surface Tension Modeling

Masanori Suzuki

Associate Professor, Osaka University, Suita, Osaka 565-0871, Japan.

Email: suzuki@mat.eng.osaka-u.ac.jp

Keywords: surface tension, slag, surface relaxation, soft X-ray absorption, molecular dynamics

ABSTRACT

Although several models for the surface tension of molten oxide slag have been proposed, suitably accurate predictions of this property are not yet possible. The surface tension, or surface excess free energy, of molten oxides is largely determined by the ionic coordination induced by surface relaxation. However, the associated mechanism of surface structural relaxation for molten oxide mixtures such as slag is complex and not yet fully understood. To allow a better evaluation of surface relaxation characteristics, the present work analysed the ionic coordination associated with the surface-relaxed states of several oxide mixtures. This work especially focused on calcium aluminate slags because these materials exhibit complex relationships between composition and surface tension. The effects of incorporating low concentrations of SiO_2 as a surface active component on the surface ionic coordination were also examined. X-ray absorption techniques were used to assess oxygen and cationic elements in glassy samples after surface relaxation treatments, and molecular dynamics simulations based on a polarisable ion model of molten slag with vacuum/melt interfaces were also performed. The X-ray absorption techniques provided data related to electron yields (which are primarily associated with surface features) and fluorescence yields (which evaluate the bulk material). Thus, the ionic coordination characteristics of both regions were investigated. The results of molecular dynamics calculations allowed statistical analysis of the distributions of Al- or Si-centred polymorphs as well as the bond angles between cations and oxygen anions in the vacuum-exposed and bulk regions in the equilibrated melt. The results indicated that bridging oxygen ions were preferentially distributed in the relaxed surface region rather than non-bridging oxygens. These bridging oxygen ions represented vertex connections between AlO_4 or SiO_4 tetrahedra. In the case of the calcium aluminate slags, the addition of one Ca^{2+} ion as charge compensation for two Al^{3+} ions was found to be necessary to form two AlO_4 tetrahedra. This specific feature of surface ionic coordination could be responsible for the complex trends observed in surface tension data. The incorporation of low concentrations of SiO_2 reduced the proportion of tetrahedrally-coordinated Al ions such that higher coordination states become dominant in the bulk of the material, whereas AlO_4 tetrahedra were preferentially distributed in the surface region. SiO_4 tetrahedra were the preferred Si-centred polymorph and were likely connected to one another to form bridging oxygen ions at the surface. On the basis of these results, a model to predict slag surface tension was proposed, and the energy of the formation of the ionic clusters resulting from surface relaxation was taken into account.

INTRODUCTION

Surface tension is one of the most important physical properties of molten slag and can affect interfacial phenomena during the processing of various materials at high temperatures. As an example, the Marangoni flow of slag, which is driven by localised changes in surface tension, can result in the local loss of furnace wall refractory materials by dissolution (Mukai, 1998). The slag-forming behaviour during refining processes² is also significantly affected by the surface tension of the molten slag (Luz, 2018). Hence, it is vital to control surface tension so as to maximise productivity and quality as well as to reduce the cost of maintaining furnace wall materials. This control will, in turn, require an understanding of surface properties, particularly the effect of the slag composition on such parameters.

The surface tension of a liquid is related to the surface free energy per unit area, which can be considered equivalent to the excess energy generated by the incomplete bonding of surface atoms

(Tanaka, 1996). Consequently, surface tension typically increases as the bonding energy between atoms increases. However, this rule cannot be applied to the surface tension properties of molten oxides. As an example, the relationship between the surface tension of a pure molten oxide at its melting point and the cationic potential ($U = Z/r$, where Z is the valence of the cation and r is the ionic radius of the cation) (King, 1951) does not show a simple trend. MnO, which has a moderate cationic potential, exhibits the highest surface tension among pure molten oxides, whereas SiO₂, with a high cationic potential, shows a low surface tension.

The surface tension of molten oxides strongly depends on the ionic coordination in the surface region induced by surface structural relaxation. In the case of unary oxides, oxygen ions are thought to occupy the surface region because these are larger than the corresponding cations. As such, the coordination between oxygen ions and cations can be modified to decrease the surface excess energy caused by incomplete bonding (Livey, 1956). However, in molten oxide mixtures such as slags, the surface structural relaxation mechanism is much more complex and is not yet fully understood. Although several models that partially account for surface modification have been proposed for the prediction of the surface tension of ionic melts or molten slag (Tanaka, 1998; Lee, 2002), the relationship between surface relaxation and the surface tension of molten slag has not been explored in detail. Hence, the effect of composition on the surface tension of certain oxide systems remains unpredictable. Thus, the precise prediction of surface tension will require more data concerning the surface structural relaxation mechanism in molten oxide slags.

The present work analysed the ionic coordination structures within the surface regions of molten oxide slags, taking into account surface structural relaxation. This work examined two specific cases. First, the surface ionic structure of an Al₂O₃–CaO slag, for which surface tension is minimised at an intermediate composition, was examined. Second, the effect of incorporating a low concentration of SiO₂, a surface active agent, on the surface ionic structure of the Al₂O₃–CaO slag was assessed. Two novel approaches were employed, consisting of soft X-ray absorption spectroscopy to assess oxygen and cationic elements in glassy materials with relaxed surfaces, and molecular dynamics (MD) simulations of oxide mixture melts with vacuum/melt interfaces.

EXPERIMENTAL

X-RAY ABSORPTION SPECTROSCOPY

X-ray absorption near edge structure (XANES) spectroscopy was used to determine the chemical valence values and coordination states of the target elements. In the case of this technique, the surface electrons generate an electrical current that reflects the number of such electrons and is also surface-dependent (providing information to depths of several to tens of nm from the sample surface). In contrast, monitoring the X-ray fluorescence intensity provides information concerning the bulk of the specimen (to depths of more than several tens of μm). Thus, it is possible to separately analyse the coordination states of ions in the surface and bulk regions using these two techniques. Such analyses are normally conducted at room temperature and under a high vacuum to minimize X-ray scattering by gaseous species.

The work reported herein employed oxide glasses instead of high-temperature melts based on the assumption that the surface ionic structure of the glass following structural relaxation would be similar to that of the corresponding melt. During the annealing of a crushed oxide glass sample, relaxation of the surface ionic structure takes place so as to reduce the surface excess energy caused by partially incomplete ionic bonding, similar to the mechanism proposed for the surface relaxation of an ionic melt (Tanaka, 1998). **Table 1** summarises the chemical compositions of the glass samples. Each specimen was prepared by first calcining a special grade chemical of CaCO₃ at 1223 K in air overnight to form CaO. Following this, special grades of Al₂O₃ and SiO₂ were combined with this CaO (with all materials in the powdered state), and the mixture was pressed into a pellet by applying a pressure of 10 MPa for 15 min. The resulting pellet was cut into pieces with diameters in the range of 1–2 mm, after which each piece was melted by laser irradiation. This irradiation was performed in conjunction with aerodynamic levitation to enable effective melting of the oxide samples without contamination from the container. The melting step was followed by quenching into a glassy state via rapid cooling. During this process, each slag sample was levitated and melted at 2073–2273 K, subsequently held at 1873–1973 K for 10 min, and then quenched by

turning the laser power off. The cooling rate was greater than -500 K/s during the latter stage. The resulting glass samples were annealed at 873 K for 24 h to adjust any structural distortion, after which each specimen was crushed into a powder to produce a large surface area with incomplete surface relaxation. Each glass sample was subsequently annealed again at 873 K for 48 h to promote surface structural relaxation. The annealing temperature during this step was lower than the glass transition temperature of the material to avoid crystallisation of the sample during the annealing.

TABLE 1 – Chemical compositions of the glass samples assessed in the present study

Sample name	Composition [mol%]		
	Al ₂ O ₃	CaO	SiO ₂
A1	30	70	0
A2	36.8	63.2	0
A3	50	50	0
B1	35	60	5
B2	33.2	56.8	10
B3	29.5	50.5	20

The soft X-ray absorption analyses were performed at the Ritsumeikan University SR Centre (Shiga, Japan). The powdered glass samples and the reference materials, including SiO₂ glass, α -Al₂O₃, and Mayenite (Ca₁₂Al₁₄O₃₃) crystals, were each separately attached to a pure indium plate on the sample holder to support electrical conduction, after which the holder was placed in a sealed chamber. These preparations were performed in a glovebox under Ar to avoid the absorption of moisture by the specimens. The sample chamber was subsequently attached to the soft X-ray absorption spectroscopy instrumentation, and the analyses were performed under a high vacuum of less than 10^{-6} Pa. The O K-edge XANES spectra were obtained in both the partial electron yield and partial fluorescence yield (PFY) modes using a diffraction grating with 1200 lines/mm. The Al and Si K-edge XANES spectra were obtained in the total electron yield and PFY modes using KTiOPO₄ (011) and InSb (111) dispersive crystals. The latest version of the Athena program was employed to draw the background lines using a spline function and to normalise the spectra.

MOLECULAR DYNAMICS SIMULATIONS

Classical MD calculations based on a polarisable ion model (PIM) were performed to simulate the ionic distributions in the oxide melts, including vacuum/melt interfaces. This PIM evaluated the dipole moment between each ion, μ_i , based on the polarisation parameter α_i and the electric field E_i formed at the position of the focused ion by the charges and dipoles ($\mu_i = \alpha_i \cdot E_i$) (Ishii, 2016). The potential energy function was decomposed into four parts, comprising the charge, dispersion, repulsion, and polarisation terms, expressed as:

$$\phi_{\text{Total}} = \left(\frac{q_i q_j}{r_{ij}} \right) + \left(-\sum_{i < j} \left[f_6^{ij} \frac{c_6^{ij}}{(r_{ij})^6} + f_8^{ij} \frac{c_8^{ij}}{(r_{ij})^8} \right] \right) + \left(\sum_{i < j} A_{ij} e^{-B_{ij} r_{ij}} \right) + \left(\sum_{i < j} \left[\frac{q_i r_{ij} \mu_j}{r_{ij}^3} f_4^{ij} - \frac{\mu_i \cdot q_j r_{ij}}{r_{ij}^3} f_4^{ij} + \frac{\mu_i \cdot \mu_j}{r_{ij}^3} - \frac{3(r_{ij} \cdot \mu_i) \cdot (r_{ij} \cdot \mu_j)}{r_{ij}^5} \right] + \frac{|\mu_i|^2}{2\alpha_i} \right). \quad (1)$$

The polarisation term consists of charge–dipole, and dipole–dipole interactions as well as the energy required to deform the electric fields of ions. The parameters for the PIM force field were determined to reproduce the force and dipole moment acting on each ion, which was calculated using first-principles MD calculations for identical oxide systems in the glassy and molten states.

The computation methodology employed in this work is illustrated in **Figure 1**. Initially, a cubic cell containing approximately 3000 atoms was held at 2273 K for 30,000 steps (where 1 step = 1 fs) and

then equilibrated at 2073 K for 30,000 steps, using a rigid-ion model (RIM) that neglected the polarisation term in the potential energy function. The cell was subsequently equilibrated for 100,000 steps using the PIM so as to achieve a steady value for the total cell energy. Next, the ionic configuration was extended by a factor of from three to six in one direction, and the system was again equilibrated at 2073 K in the same manner as described above. Following this, vacuum spaces were inserted in the upper and lower sides of the rectangular cell to form vacuum/melt interfaces, and the cell was equilibrated using a RIM and PIM. All these calculations were performed in the *NVT* ensemble and using the program code made by the PIM developer (Ishii, 2016). Note that, in the present MD simulations, the effects of gas molecules on the surface structure of the oxide melt were regarded as negligible.

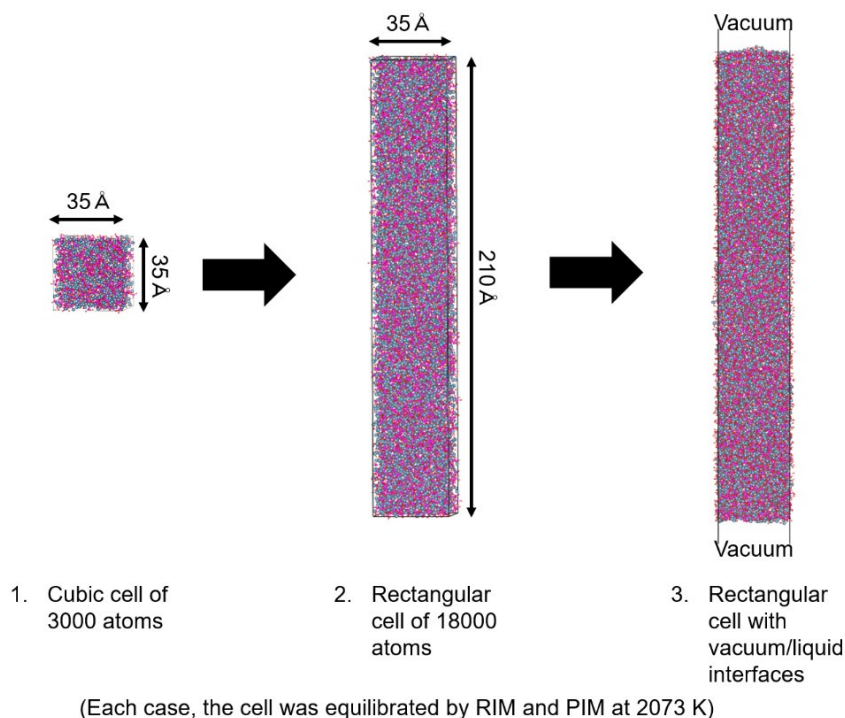


FIG 1 – Schematic diagram summarising the MD simulation procedure.

The ionic coordination between oxygen ions and cations in the equilibrated cell was analysed using the tetrahedral order parameter q (Errington, 2001), calculated according to the equation:

$$q = 1 - \frac{3}{8} \sum_{j=1}^{n-1} \sum_{k=j+1}^n \left(\cos \theta_{ijk} + \frac{1}{3} \right)^2, \quad (2)$$

where θ_{ijk} is the angle formed between the central cationic atom, denoted by j , and its neighbouring oxygen atoms, denoted by i and k . The equilibrated rectangular cell with vacuum/liquid interfaces was divided into several layers, each approximately 2 nm in thickness, and the distributions of Si- or Al-centred polymorphs were analysed for the upper and lower layers exposed to the vacuum spaces (corresponding to the surface region) and middle layers (corresponding to the bulk region).

RESULTS AND DISCUSSION

Local structure analyses

Al₂O₃-CaO system

Figure 2a presents the O K-edge XANES spectra obtained from the $\text{Al}_2\text{O}_3\text{-CaO}$ glass samples (A1–A3 in **Table 1**) after annealing to promote surface structural relaxation. Each of these spectra exhibits two broad absorption peaks (labelled a or a' and b). According to Henderson (2007), peaks a and a' correspond to Al–O–Ca non-bridging oxygen (Al–NBO), whereas peak b corresponds to Al–O–Al bridging oxygen (Al–BO). Al^{3+} ions in these glasses are thought to have primarily had tetrahedral coordination states. In the case of the surface spectrum, the intensity of the Al–BO peak (that is,

peak b) is higher than that of the Al–NBO peak (a'). In the range of 30–50 mol% Al₂O₃, this trend becomes more pronounced with increases in the Al₂O₃ content. In contrast, the intensities of these two peaks are comparable in the bulk spectra, and there is no significant effect of composition. These results indicate that Al–BO was preferentially situated at the surface rather than in the bulk of the glass. For glasses A1 and A2, the positions of the Al–NBO peaks (a') in the surface spectra are negatively shifted relative to those in the bulk spectra (a). This change may have resulted from the differences in oxygen coordination to Ca²⁺ ions between the surface and bulk regions, which in turn was related to the energy required for core electron transitions (Jiang, 2006).

Figure 2b shows the Al K-edge XANES spectra of the Al₂O₃–CaO glass samples after surface structural relaxation. Two absorption peaks (c at 1565 eV and d at 1568 eV) can be seen, corresponding to Al³⁺ cations that are tetrahedrally and octahedrally coordinated with oxygen anions, respectively (Kato, 2001). In the surface spectra, the intensity of peak c is obviously increased compared with that of peak d as the Al₂O₃ content increases, while the ratio of the c and d peak intensities in the bulk spectra varies only minimally. From these data, it appears that tetrahedral coordination was preferred for Al³⁺ ions in the surface region, particularly with increasing Al₂O₃ content. In this case, BO ions could be formed by the connection of two AlO₄ tetrahedra. However, it should be noted that one Ca²⁺ cation had to be supplied in conjunction with the formation of every two AlO₄ tetrahedra for charge compensation. Therefore, the connection of dual AlO₄ tetrahedra was possible only at intermediate compositions within the Al₂O₃–CaO system.

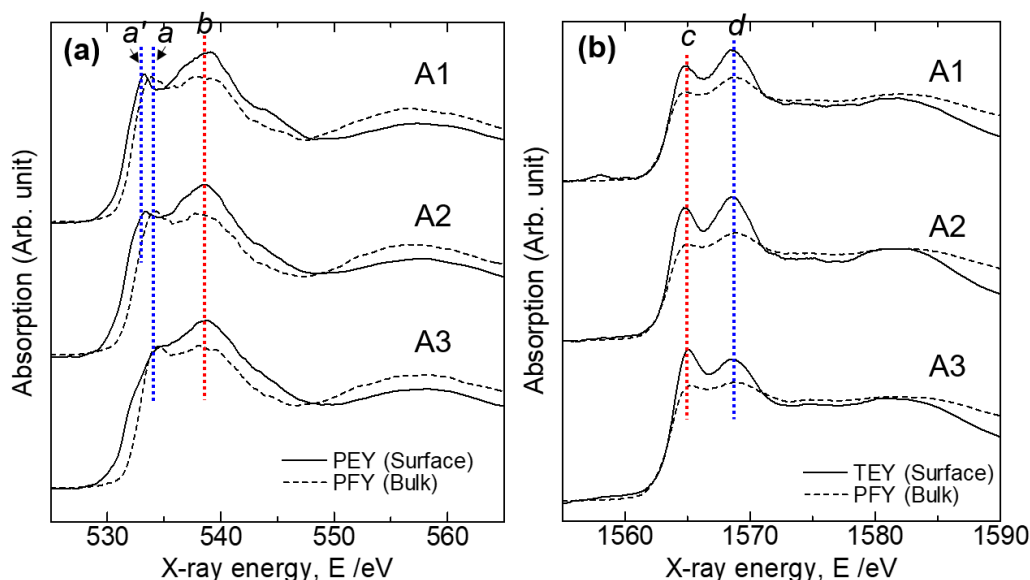


FIG 2 – (a) O K-edge and (b) Al K-edge XANES spectra of Al₂O₃–CaO glass (samples A1–A3) after annealing for surface structural relaxation.

Al₂O₃–CaO–SiO₂ system

Figure 3a shows the O K-edge XANES spectra of the Al₂O₃–CaO–SiO₂ glass samples (B1–B3) after annealing for surface relaxation. Similar to the results obtained from the Al₂O₃–CaO glass specimens, a negative shift in the NBO absorption peak position in the surface region (e') compared with that in the bulk region (f) is apparent. In the case of the surface spectra, the intensity of the BO absorption peak (f) is higher than that of the NBO peak (e'), regardless of the SiO₂ content. With increases in the SiO₂ content, the location of the BO peak in the surface spectra (f') shifts negatively and approaches the peak corresponding to (Si–O–Si) BO (f'') in the spectrum of the silica glass. This finding demonstrates that Si cations partially contributed to the formation of BO ions in the surface region.

Figure 3b presents the Al K-edge XANES spectra obtained from the Al₂O₃–CaO–SiO₂ glasses after surface structural relaxation. These spectra contain two absorption peaks corresponding to AlO₄ (c) and AlO₆ (d) coordination states. With increases in the SiO₂ content, the intensity of the AlO₄ peak in the surface spectra can be seen to greatly increase and eventually exceed those of the AlO₆ peaks. Thus, it appears that the AlO₄ coordination state was selectively distributed throughout the

surface region when increasing the SiO₂ content. Conversely, the bulk spectra show no change in the intensity ratio of these two peaks.

Figure 3c shows the Si K-edge XANES spectra acquired from the Al₂O₃–CaO–SiO₂ glasses after surface structural relaxation. The bulk spectra clearly exhibit two absorption peaks (g and h). The peak g corresponds to that observed for grossular (Ca₃Al₂[SiO₄]₃) crystals in which SiO₄ tetrahedra are surrounded by AlO₆ octahedra through NBO (Si^{IV}–O–Al^{VI}). The other peak (h) indicates the presence of octahedrally coordinated Si cations in silicon phosphate (SiP₂O₇). Thus, while SiO₂ was a minor component in these glasses, Si cations evidently had both tetrahedral and octahedral coordination states in the bulk region. In contrast, the surface spectrum shows only one broad absorption peak. As the SiO₂ content was increased, the central peak can be seen to approach the peak (i) associated with anorthite (CaAl₂Si₂O₈) crystals, in which SiO₄ tetrahedra are connected to AlO₄ tetrahedra through BO (Si^{IV}–O–Al^{IV}). These results confirm that the dominant coordination state in the surface region changed from Al^{IV}–O–Al^{IV} to Si^{IV}–O–Al^{IV} following the addition of a small amount of SiO₂, although both states involved BO.

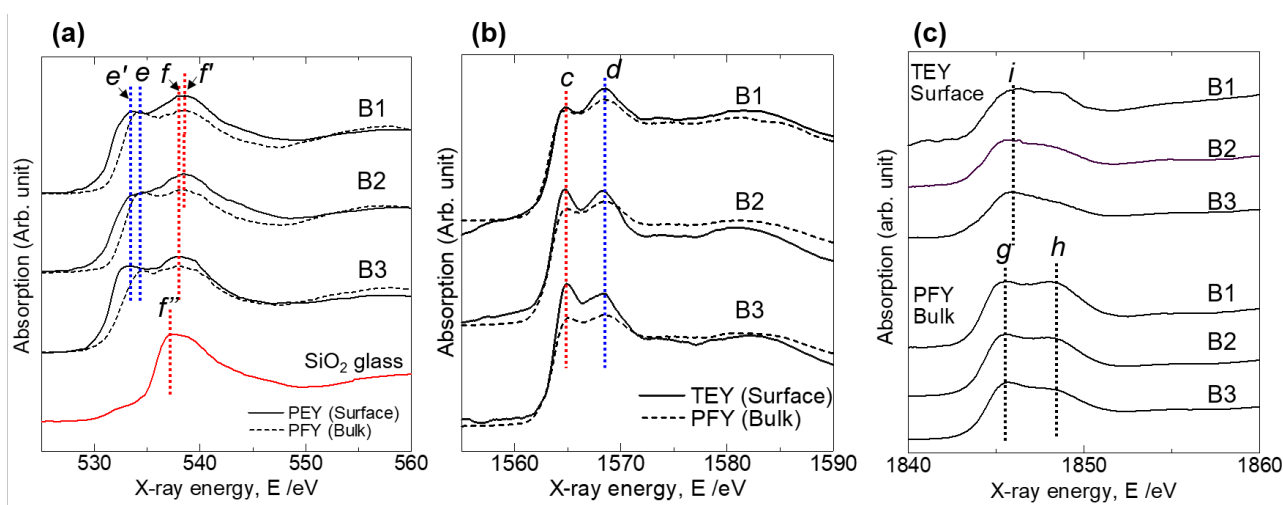


FIG 3 – (a) O K-edge, (b) Al K-edge and (c) Si K-edge XANES spectra obtained from Al₂O₃–CaO–SiO₂ glass specimens (B1–B3) after annealing for surface structural relaxation.

MD simulations of ionic configurations

Al₂O₃-CaO system

This study examined melts having the compositions 25Al₂O₃–75CaO and 50Al₂O₃–50CaO (mol%).

Figure 4a shows the distribution of Al-centred polymorphs in different layers throughout an equilibrated cell having vacuum/melt interfaces for the former in the molten state, based on the *q* parameter as expressed in Eq. (2). Three different Al–O coordination states (AlO₄, AlO₅, and AlO₆) were identified in this material. The proportion of the AlO₄ coordination state was slightly higher than average in the surface layers, whereas those of the AlO₅ and AlO₆ states were lower. In contrast, the bulk region exhibited a lower proportion of AlO₄ but higher proportions of AlO₅ and AlO₆ than average. These data indicate that tetrahedral coordination was preferred in the surface layer.

Figure 4b summarises the distribution of Al-centred polymorphs in the equilibrated 50Al₂O₃–50CaO (mol%) melt cell with vacuum/melt interfaces. As the Al₂O₃ content was increased, AlO₅ became the dominant coordination state in the bulk layer rather than AlO₄. However, these results clearly demonstrate that AlO₄ was preferentially distributed in the surface layers.

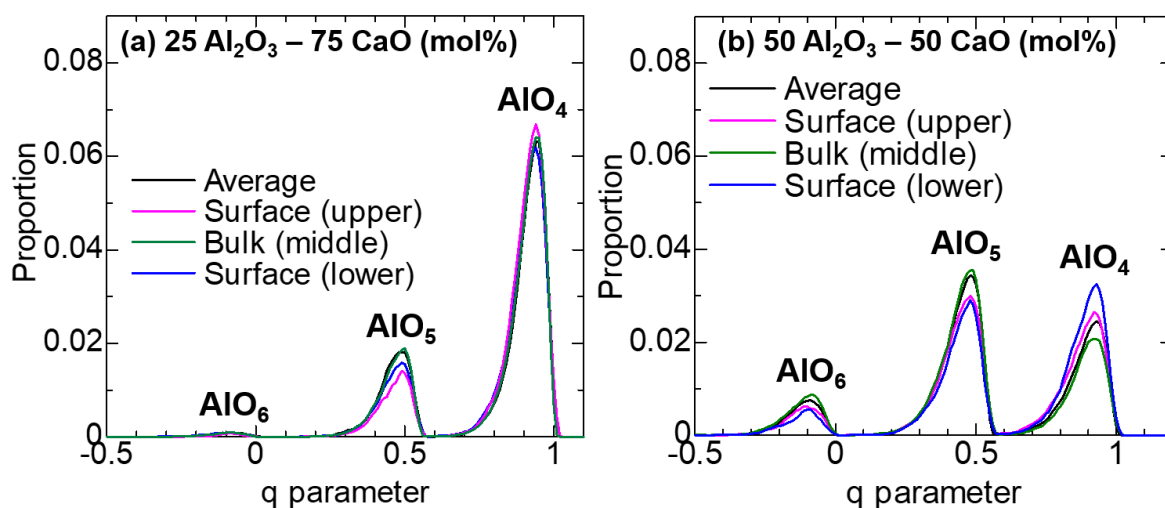


FIG 4 – Distributions of Al-centered polymorphs in the cells of Al_2O_3 -CaO melts with vacuum/melt interfaces equilibrated at 2073 K. (a) $25\text{Al}_2\text{O}_3$ - 75CaO (mol%) and (b) $50\text{Al}_2\text{O}_3$ - 50CaO (mol%).

Connections among the Al-centered polymorphs were examined by analysing the distributions of Al–O–Al bond angles. **Figure 5a** shows the result for the $25\text{Al}_2\text{O}_3$ - 75CaO (mol%) melt, while **Figure 5b** presents the data for the $50\text{Al}_2\text{O}_3$ - 50CaO (mol%) melt. In both cases, two broad peaks can be seen. The first, θ_1 , is located at approximately 100° and corresponds to the edge connections between pairs of polymorphs via two oxygen anions. The other, θ_2 , is situated at approximately 125° and corresponds to vertex connections between pairs of tetrahedra through single BO ions. The surface layers produced a more intense θ_2 peak but a less intense θ_1 peak compared with the averages and the peak intensities obtained from the bulk layer. These data indicate that vertex connections between AlO_4 tetrahedra via single BO ions ($\text{Al}^{\text{IV}}\text{-O-Al}^{\text{IV}}$) were preferentially formed in the surface region.

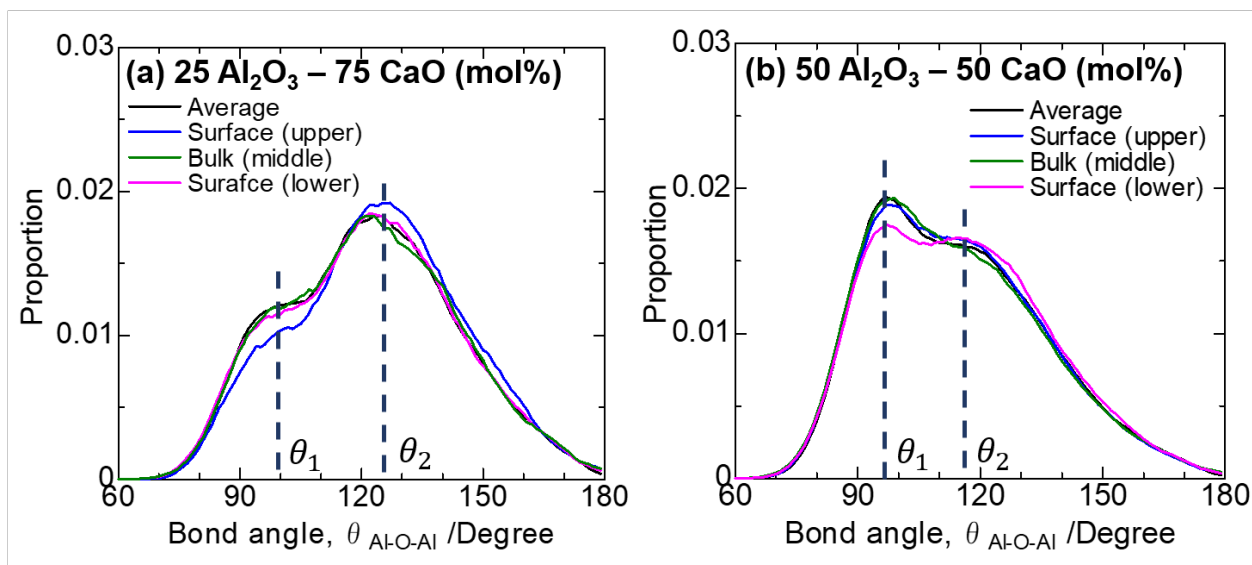


FIG 5 – Distributions of Al–O–Al bond angles in the cells of Al_2O_3 -CaO melts with vacuum/melt interfaces equilibrated at 2073 K. (a) $25\text{Al}_2\text{O}_3$ - 75CaO (mol%) and (b) $50\text{Al}_2\text{O}_3$ - 50CaO (mol%).

Al_2O_3 -CaO-SiO₂ system

Figures 6a and **6b** summarise the distributions of SiO_n polymorphs in different layers for the trials in which 5 and 20 mol% SiO_2 were added to the $37\text{Al}_2\text{O}_3$ - 63CaO (mol%) melt, respectively. A SiO_2 content of 5 mol% generated various types of Si–O coordination, although the octahedral state was dominant. The proportion of SiO_4 tetrahedra was slightly higher in the surface layers, whereas the amounts of other polymorphs were lower compared with the bulk layer. At a SiO_2 concentration of

20 mol%, the SiO_4 tetrahedra became dominant, and no specific differences were observed between the surface and bulk layers.

The distributions of AlO_n polymorphs in the surface and bulk layers are shown in **Figures 7a** and **7b**. At a SiO_2 content of 5 mol%, the AlO_n distributions in the surface and bulk layers were comparable. However, after the SiO_2 concentration was adjusted to 20 mol%, AlO_4 tetrahedra were preferentially located in the surface layer rather than AlO_5 or AlO_6 .

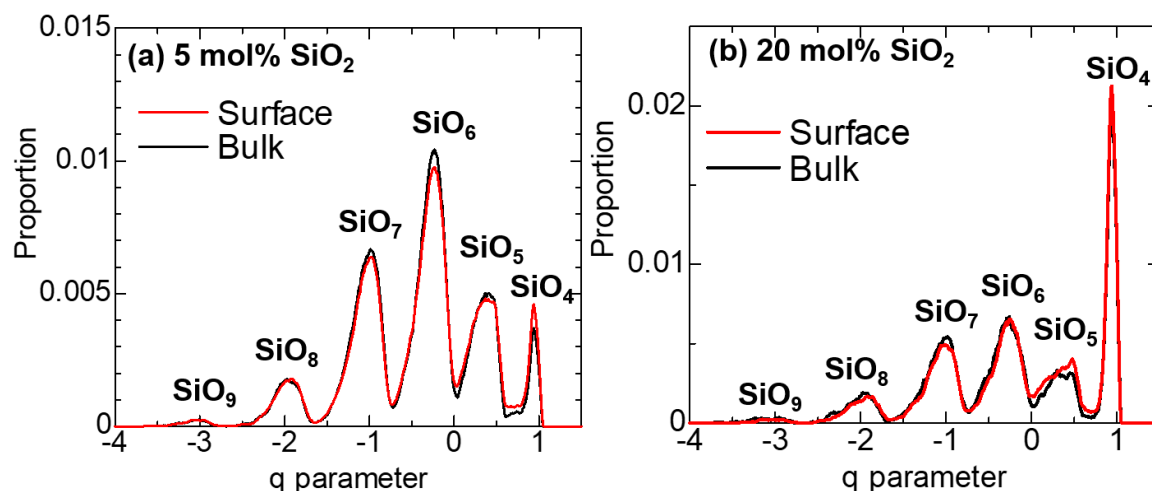


FIG 6 – Distributions of Si-centred polymorphs in the cells of Al_2O_3 - CaO - SiO_2 melts with vacuum/melt interfaces equilibrated at 2073 K. (a) 5 mol% SiO_2 and (b) 20 mol% SiO_2 .

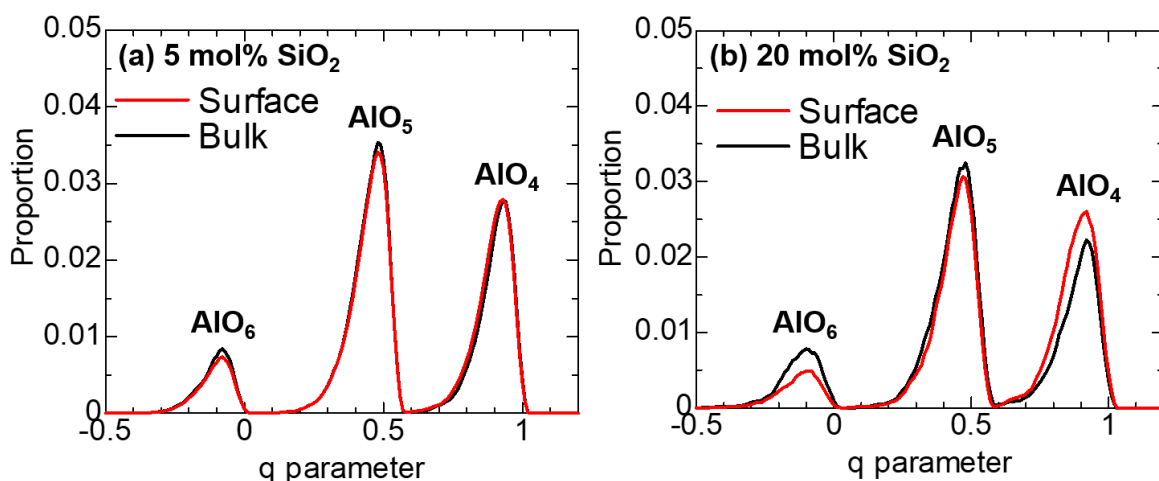


FIG 7 – Distributions of Al-centred polymorphs in the cells of Al_2O_3 - CaO - SiO_2 melts with vacuum/melt interfaces equilibrated at 2073 K. (a) 5 mol% SiO_2 and (b) 20 mol% SiO_2 .

Analyses of the connections between Si- and Al-centred polymorphs based on bond angle distributions established that vertex connections between AlO_4 and SiO_4 tetrahedra to form $\text{Si}^{\text{IV}}\text{-O-Al}^{\text{IV}}$ units via BO ions were preferentially situated in the surface region in conjunction with SiO_2 concentration of 5 mol%. This effect is demonstrated by the greater intensity of the θ_2 peak but lower intensity of the θ_1 peak in the surface region compared with the bulk (see Fig. 8(a)). The above results clearly indicate that the incorporation of a small amount of SiO_2 significantly affected the distribution of AlO_n in the melt. In particular, AlO_4 and SiO_4 tetrahedra were preferentially distributed in the surface region, some of which contributed to the formation of BO ions such as $\text{Si}^{\text{IV}}\text{-O-Si}^{\text{IV}}$, $\text{Al}^{\text{IV}}\text{-O-Si}^{\text{IV}}$ and $\text{Al}^{\text{IV}}\text{-O-Al}^{\text{IV}}$. This trend is consistent with the results obtained using XANES spectroscopy to assess the quenched Al_2O_3 - CaO - SiO_2 glasses with surface structural relaxation.

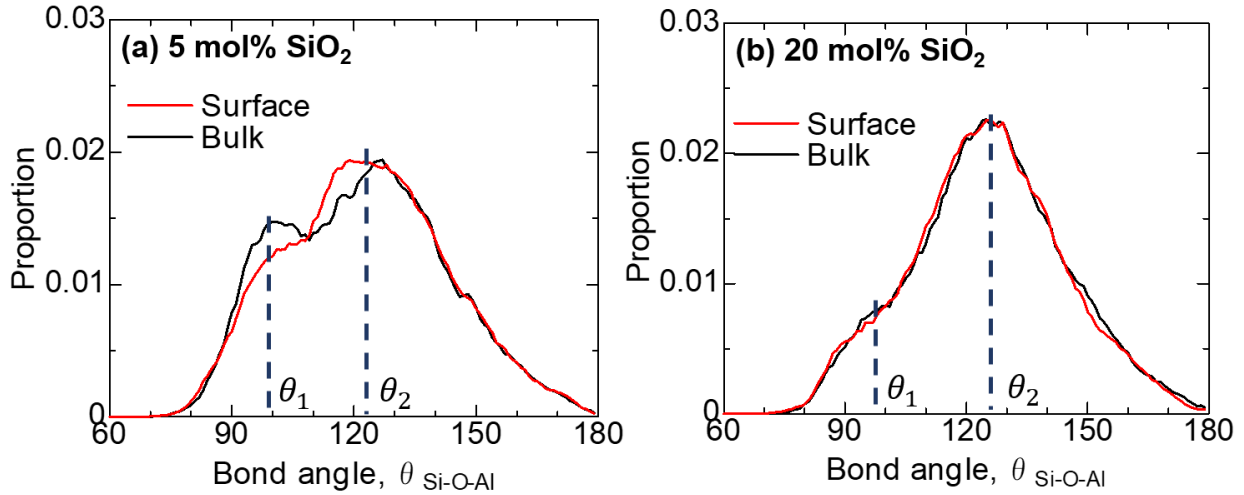


FIG 8 – Distributions of Si–O–Al bond angles in the cells of $\text{Al}_2\text{O}_3\text{-CaO-SiO}_2$ melts with vacuum/melt interfaces equilibrated at 2073 K. (a) 5 mol% SiO_2 and (b) 20 mol% SiO_2 .

Modeling the surface tension of molten slag

The results obtained from XANES spectroscopy of the glass specimens after surface structural relaxation and the MD simulations of the melt structures with vacuum/melt interfaces both indicated that BO ions were preferentially formed in the surface region. This phenomenon was associated with the selective distribution of AlO_4 or SiO_4 tetrahedra with vertex connections. Because these tetrahedra formed strong covalent bonds with the nearest cations, the distribution of BO ions significantly decreased the surface excess energy, which in turn was related to the surface tension. This trend is believed to explain the surface structural relaxation of molten aluminosilicate slags.

On the basis of the analyses of surface structural relaxation described above, a novel model for predicting the surface tension of molten slag can be proposed. Based on the fundamental equation (Butler, 1932) used to predict the surface tension of a liquid solution, the surface tension of a slag in which oxygen ions are bonded to two different cations i and j ($i\text{-O-}j$, described as ij) to form structural units can be calculated as:

$$\sigma = \sigma_{ij} + \frac{RT}{A_{ij}} \ln \frac{X_{ij}^{\text{Surface}}}{X_{ij}^{\text{Bulk}}} + \frac{1}{A_{ij}} \left\{ \left[\begin{array}{l} \text{Difference in energy of formation} \\ \text{of ionic clusters between} \\ \text{surface and bulk regions} \end{array} \right] + \left[\begin{array}{l} \text{Difference in energy of energy} \\ \text{of connected chain structures} \\ \text{between surface and bulk} \end{array} \right] \right\}. \quad (3)$$

In the above equation, σ_{ij} is the surface tension of pure component, A_{ij} is the molar area of the melt comprising $i\text{-O-}j$ structural units, and X_{ij}^{Surface} and X_{ij}^{Bulk} are the mole fractions in the surface and bulk regions, respectively. Thus, the surface tension of an oxide melt can vary with the relative proportions of the structural units (such as $\text{Si}^{\text{IV}}\text{-O-Si}^{\text{IV}}$ or $\text{Al}^{\text{IV}}\text{-O-Al}^{\text{IV}}$) in the surface and bulk regions. Surface tension can also be affected by differences in the partial interaction energies of these structural units (that are, in turn, related to their connecting states in the short and middle-order ranges) between the surface and bulk regions. The partial interaction energies of the structural species in the surface region are being evaluated, and modeling of the effect of structural relaxation on the surface tension of oxide slag will be studied in the future by the author.

CONCLUSIONS

Structural analyses of the relaxed surfaces of molten calcium aluminosilicate slags were conducted based on soft X-ray absorption spectroscopy of quenched glass samples after surface structural relaxation and MD simulations of ionic configurations of oxide melts with vacuum/melt interfaces. The results obtained from these two techniques were consistent with one another and established that BO ions were preferentially formed in the surface region by vertex connections between Al- or Si-centred polymorphs. In the case of the $\text{Al}_2\text{O}_3\text{-CaO}$ system, Al^{3+} ions tetrahedrally-coordinated

with oxygen ions (AlO_4 or Al^{IV}) were preferentially distributed in the surface region, and some such units were connected through BO ions ($\text{Al}^{\text{IV}}\text{--O--Al}^{\text{IV}}$). However, it should be noted that Ca^{2+} ions were required for the purpose of charge compensation for Al^{3+} ions when generating the AlO_4 tetrahedra. Hence, this ionic configuration occurred at the intermediate composition. The incorporation of a minor amount of SiO_2 in the calcium aluminate slag greatly changed the ionic coordination states in the surface region. Tetrahedral coordination states with oxygen ions (SiO_4 or Si^{IV}) were preferentially situated in the surface region. Additionally, the incorporation of SiO_2 resulted in the segregation of AlO_4 in the surface region while the proportions of AlO_5 and AlO_6 in the bulk were increased. These structures partially combined with one another at their vertexes to form BO ions (that is, $\text{Al}^{\text{IV}}\text{--O--Si}^{\text{IV}}$). Based on these findings, a new model was constructed that allows the surface tension of molten slags to be predicted.

ACKNOWLEDGEMENTS

This work was financially supported by the Japan Society for the Promotion of Science through a KAKENHI Grant-in-Aid for Scientific Research (no. JP21H01683). The soft X-ray absorption analyses were performed under projects nos. S19010, S20003 and S22016 with the support of the Ritsumeikan University SR Center (Shiga, Japan). Molecular dynamics simulations were conducted at the Research Center for Computational Science, Okazaki, Japan, under project nos. 21-IMS-C097, 22-IMS-C097 and 23-IMS-C084. The author is grateful to Dr. Norimasa Umesaki (previously at Osaka University, Japan) for suggestions regarding both the X-ray absorption analyses and molecular dynamics simulations. In addition, the author wishes to thank Assoc. Prof. Yoshiki Ishii (Kitasato University, Japan) and Mr. Yusuke Asano (Osaka University, Japan) for supporting the computational and experimental studies.

REFERENCES

- Butler, J A V, 1932. The thermodynamics of the surfaces of solutions. *Proc. R. Soc. Lond. A*, 135:348–375.
- Choi, J Y and Lee, 2002. Thermodynamic Evaluation of the Surface Tension of Molten $\text{CaO--SiO}_2\text{--Al}_2\text{O}_3$ Ternary Slag. *ISIJ Int.*, 42(3):221-228.
- Errington, J R, Debenedetti, P G, 2001. Relationship between structural order and the anomalies of liquid water. *Nature*, 409:318-321.
- Henderson, G S, Neuville, D R and Cormier, L, 2007. An O K-edge XANES study of calcium aluminates. *Canad. J. Chem.*, 85:801-805.
- Ishii, Y, Salanne, M, Charpentier, T, Shiraki, K, Kasahara, K and Ohtori, N, 2016. A DFT-Based Aspherical Ion Model for Sodium Aluminosilicate Glasses and Melts. *J. Phys. Chem. C*, 120:24370-24381.
- Jiang, N, 2006. Structure and composition dependence of oxygen K edge in CaAl_2O_4 . *J. Appl. Phys.*, 100:013703.
- Kato, Y, Shimizu, K, Matsushita, N, Yoshida, T, Yoshida, H, Satsuma, A and Hattori, T, 2001. Quantification of aluminium coordinations in alumina and silica-alumina by Al K-edge XANES. *Phys. Chem. Chem. Phys.*, 3:1925-1929.
- King, T B, 1951. The surface tension and structure of silicate slags. *J. Soc. Glass Technol.*, 35:241-259.
- Livey, D T and Murray, P, 1956. Surface Energies of Solid Oxides and Carbides. *J. Am. Ceram. Soc.*, 39(11):363-372.
- Luz, A P, Tomba Martinez, A G, López, F, Bonadia, P and Pandolfelli, V C, 2018. Slag foaming practice in the steelmaking process. *Ceram. Int.*, 44(8):8727-8741.
- Mukai, K, 1998. Marangoni Flows and Corrosion of Refractory Walls. *Phil. Trans: Math. Phys. Eng. Sci.*, 356(1739):1015-1026.

- Tanaka, T, Hack, K, Iida, T and Hara, S, 1996. Application of Thermodynamic Databases to the Evaluation of Surface Tensions of Molten Alloys, Salt Mixtures and Oxide Mixtures. *Z. Metallkd.*, 87(5):380-389.
- Tanaka, T, Hara, S, Ogawa, M and Ueda, T, 1998. Thermodynamic Evaluation of the Surface Tension of Molten Salt Mixtures in Common Ion Alkali-Halide Systems. *Z. Metallkd.*, 89(5):368-374